Science Advances
AAAS

advances.sciencemag.org/cgi/content/full/6/37/eabb4112/DC1

Supplementary Materials for

Deconstructing laws of accessibility and facility distribution in cities

Yanyan Xu, Luis E. Olmos, Sofiane Abbar, Marta C. González*

*Corresponding author. Email: martag@berkeley.edu

Published 11 September 2020, *Sci. Adv.* **6**, eabb4112 (2020)
DOI: 10.1126/sciadv.abb4112

This PDF file includes:

Notes S1 to S4
Figs. S1 to S8
Tables S1 and S2
References

Notes

S1 List of variables and notations for the accessibility analysis

$Block$ Definition of blocks used in this work is derived from the LandScan dataset (*37*). The LandScan dataset has 20,880 rows and 43,200 columns covering North 84 degrees to South 90 degrees and West 180 degrees to East 180 degrees.

N Number of facilities in a city. In the *actual* scenario, the foursquare facilities of the same type within one block are merged into one; in the *optimal* scenario, a block can only accommodate at most one facility. That is, N equals to the number of blocks with facilities. Note that the amount of population served by each facility is not limited.

N_{max} Total number of blocks within the boundary of the city.

N_{occ} Number of the blocks which accommodate more residents than a predefined threshold, a.k.a. occupied blocks. In real-world cities, the threshold is set to 500, which is a typical threshold to distinguish urban and rural regions. In toy cities, the threshold is set to 50.

D Ratio between the number of facilities N and the total number of blocks N_{max} in a city, $D = N/N_{max}$.

D_{occ} Ratio between the number of facilities N and the number of occupied blocks N_{occ} in a city, $D_{occ} = N/N_{occ}$.

p_i Population in the ith block of a city. The data is from LandScan and i is the index of the block, ranging from 1 to N_{max}.

P Total population of the city, $P = \sum_{i=1}^{N_{max}} p_i$.

a_i Area of the ith block. The unit is km^2. The area is approximately 1 km^2 for blocks near the Equator.

$\bar{a}$ Average area of blocks in the city, $\bar{a} = \frac{1}{N_{max}} \sum_{i=1}^{N_{max}} a_i$.

l_{min} Travel distance in block. $l_{min} \approx 0.5 \cdot \sqrt{a_i}$. It is close to 0.5 km near the Equator.

$\hat{l}_i$ Travel distance from the ith block to the nearest facility in the road network under the *actual* scenario. The unit is km.

l_i Travel distance from the ith block to the nearest facility in the road network under the *optimal* scenario. The facilities are optimally located to minimize the total travel distance of all population. The unit is km.

r_i Gain index of the ith block. It is the ratio between the travel distance to the nearest facility in *optimal* and *actual* scenarios, $r_i = l_i/\hat{l}_i$.

$\hat{L}$ Average travel distance to the nearest facilities in the *actual* scenario, $\hat{L} = \frac{1}{P} \sum_{i=1}^{N_{max}} p_i \hat{l}_i$.

L Average travel distance to the nearest facilities in the *optimal* scenario, $L = \frac{1}{P} \sum_{i=1}^{N_{max}} p_i l_i$.

R Optimality index of a given type of facility in the city, $R = \frac{L}{\hat{L}} = \frac{\sum_{i=1}^{N_{max}} p_i l_i}{\sum_{i=1}^{N_{max}} p_i \hat{l}_i}$.

n_j^S Number of blocks in the *service community* of the jth facility. j is the index of facility, ranging from 1 to N.

$n_{j,occ}^S$ Number of occupied blocks with population above a threshold in the *service community* of the jth facility. $n_{j,occ}^S \leq n_j^S$.

a_j^S Area of the *service community* of the jth facility, $a_j^S \approx n_j^S \cdot \bar{a}$. The unit of a_j^S is km^2.

$a^S_{j,occ}$ Area of the occupied blocks in the *service community* of the jth facility, $a^S_{j,occ} \approx n^S_{j,occ} \cdot \bar{a}$. $a^S_{j,occ} \leq a^S_j$ and its unit is km^2.

p^S_j Population in the *service community* of the jth facility. It is the summation of the population of all blocks in this community.

ρ^S_j Population density in the service community of the jth facility, $\rho^S_j = p^S_j / a^S_j$. The unit of ρ^S_j is km^{-2}.

d^S_j Facility density in the *service community* of the jth facility, $d^S_j = 1/a^S_j$. The unit of d^S_j is km^{-2}.

g^S_j Geometric factor in the *service community* of the jth facility. It's introduced to estimate the average travel distance in one communinty. We assume it's a constant value in each city. That is $g^S_j \approx g_{city}$.

β Fitted exponent of the power law between facility density $\langle d^S_j \rangle$ and population density $\langle \rho^S_j \rangle$ in *service communities*, that is $d^S_j \propto (\rho^S_j)^\beta$.

α Decay rate of the share population in blocks without facilities, $1 - p(N) = e^{-\alpha N}$.

γ Fitted exponent of the power law between the number of occupied blocks $\langle n^S_{j,occ} \rangle$ and the total number of blocks $\langle n^S_j \rangle$ in *service communities*, that is $n^S_{j,occ} \propto (n^S_j)^\gamma$.

$\{A, \lambda\}$ Free parameters to calibrate in the exponential function $L(N) = 0.5 \cdot (1 - e^{-\alpha N}) + A \cdot N^{-\lambda} \cdot e^{-\alpha N}$.

$\{\kappa, \theta\}$ Free parameters in the Gamma distribution for the travel distance in the *optimal* scenario in cities. That is $f(l) = \frac{1}{\Gamma(\kappa)\theta^\kappa} l^{\kappa-1} e^{-\frac{l}{\theta}}$, where l denotes the personal travel distance from a residential place to the nearest facility.

s_i Share of population in the ith block, $s_i = p_i/P$.

$\mathcal{M}$ Distance matrix of a city for the calculation of UCI (*54*). The value of each element represents the haversine distance between the centroids of two blocks. The main diagonal of $\mathcal{M}$ is equal to zero.

V Venables index, is a spatial separation index for the calculation of UCI (*54*), $V = \mathcal{S}' \times \mathcal{M} \times \mathcal{S}$. $\mathcal{S}$ is a vector of share of population in block s_i of the city. V_{max} means the maximum attainable value of the spatial separation index, in which all population are assumed settled in the blocks on the border of the city.

UCI Urban centrality index measures the centrality of population distribution in space and is proposed by Pereira et al. (*54*). $UCI = \frac{1}{2}\sum_{i=1}^{N_{max}} \left(s_i - \frac{1}{N_{max}}\right) \cdot \left(1 - \frac{V}{V_{max}}\right)$. The larger the UCI, the more centralized is the city.

S2 Data description

S2.1 Selection of city boundary

The selection of city boundary impacts the distribution of population and the number of facilities localized in the city in reality. The definitions of urban borders depend on population and their commuting zones (*8, 57*). In this study, we use the metroplex region of each city for study. We first try to find the boundary of metroplex from the publicly available data. If the data is not available, we manually draw the boundary by including the urban area and the rural area of the city. The selected boundaries of the six cities, Boston, LA, NYC, Doha, Dubai, and Riyadh, can be observed in Fig. S1.

S2.2 Acquiring road network from OpenStreetMap

OpenStreetMap is a collaborative project to create a free editable map of the world in a crowd-sourcing way (*39*). We collect the road network in each city, including the nodes and links, using the OpenStreetMap API. Each node is associated with an ID, longitude and latitude; each edge is associated with the length, the start and end node IDs. To calculate the shortest path between two blocks, we first randomly selects a node in each block and find the shortest path in distance between them in the road network using the Dijkstra algorithm. For a fast calculation of the shortest travel distance, we remove the residential roads from our network. The final road networks of the six cities are shown in Fig. S1.

S2.3 Foursquare facility data

The facility data were collected from the Foursquare API (*40*), a location based service mobile app which provides the information and personalized recommendations of places to users using their checked-in locations. The data of each city are collected within its boundary, as shown in Fig. S1. Each facility is associated with its geographic location and two classes corresponding to two levels. We name the lower level class as the category of facility (e.g., medical center, college & university) and the high level class as the type of facility (e.g., hospital, middle school) in this paper. The spatial distribution of collected facilities in the 6 cities are presented in Fig. S1. They are grouped into 9 categories, as shown in the legend.

S3 On the optimality index

To comprehensively assess the planning of facilities under a given planning scenario, we define the *optimality index*, R, which equals to the ratio between the optimal average travel distance L and the travel distance achieved by the actual planning scenario $\hat{L}$. Apparently, $R \in (0, 1]$ and $R = 1$ when the facilities are optimally distributed, minimizing the total travel cost of all population to their facilities. Larger values of R indicate better localization of facilities in space. We design two extreme strategies for facility assignment, namely *random* assignment and *population-weighted* assignment, and compare their optimality indices with the planning in reality, i.e. *actual* scenario. For each facility assignment strategy, only one facility is allowed to localize in one block. That is, once a facility is assigned to a block, this block is excluded for the next trial.

- *Random* assignment (population blind): Facilities are distributed randomly in the city among the N_{max} blocks. Population distribution and the accessibility of residents are neglected.
- *Population-weighted* assignment: Facilities are distributed proportionally to the share of population in blocks. To that end, we define one probability for each block, normalizing the population in the block by the total population in all available blocks.

We then calculate the average travel distance of all population from their residential block to the nearest facility. We expect the following: (1) The locations of facilities in *actual* scenario should give travel distances that lie in between the travel distances given by the two extreme assignment strategies due to the following reasons: *random* assignment always produces the largest travel cost due to lack of information on population; the simple *population-weighted* assignment performs better than the *actual* scenario mainly because of the difficulty and expenses that a relocation entails along with the evolution of population distribution. (2) Monocentric cities would achieve better R score in the *population-weighted* strategy than polycentric cities. For polycentric cities (sprawled), the two extreme assignment strategies should give similar travel distances.

The above conjectures are confirmed with the simulation results in the six cities, as shown in Fig. S4C. We simulate the two extreme strategies by assigning the same number of facilities as the actual number of the 10 types of facilities, as well as some large numbers in the five cities except NYC (the number of facilities in *actual* scenario is large enough), to investigate the change tendency of the R score along with the ratio between N and N_{max}. In each panel of Fig. S4C, the light and dark gray markers represent the R score of the *population-weighted* and *random* assignment strategy, respectively. The colored markers represent the R score of the actual distribution of 10 types of facilities, e.g., hospitals, banks, fire stations. For intermediate values of N/N_{max}, Fig. S4C shows that the population-weighted assignment strategy gives R ranging from 0.6 to 0.8. As expected, for LA (polycentric), *random* and *population-weighted* assignments are similar; for Dubai (monocentric) the gap between *random* and *population-weighted* are large due to the uneven distribution of population. The R of actual distribution in Boston, Dubai, NYC are between the two limits, while R in Doha, Riyadh and LA are very close to the *random* assignment. For certain facilities, Riyadh has worst travel distances in reality than the *random* assignment. This means groups of facilities are located in the low density blocks (as our method does not allow for repeated allocation). The imbalance between facility locations and service delivery has been reported in previous studies (*53*). For practical purposes it would be interesting to identify which facilities are closer to the random scenario.

S4 Derivation of the average optimal travel distance

S4.1 Modeling travel distance with population distribution and number of facilities

In the *optimal* scenario, we assume all of the residents find the nearest facility in terms of travel distance to meet their needs. In the toy cities, due to the lack of road networks, the routing distance between two blocks equals to the Euclidian distance between their centroids. In the real cities, the routing distance is derived by randomly selecting intersections in each block and then calculating the shortest path between them in terms of distance in the road network. In this way, each facility serves one or more blocks. We define all blocks that share the same facility j as a *service community*, and denote the service area of facility j as $a_j^S \approx n_j^S \cdot \bar{a}$, where n_j^S is the number of blocks in the *service community* of the jth facility, $\bar{a}$ is the average block area in the city. Assuming the population density of each block, $\rho_i = p_i/a_i$, varies little over the typical size of the service area, one expects the average displacement from the residential location to facility to be in the order of $\overline{d_j^S} = g_j^S \cdot (a_j^S)^{0.5}$, where g_j^S is a geometric factor in the *service community* that depends on the shape of the service area. It is noteworthy that in the toy cities, we are using the Euclidian distance as the routing distance. But in the real cities, the routing distance is lager than the displacement (Euclidian distance) due to the constraints of road networks. Here we assume the routing distance is proportional to the displacement on average in one city. Thus, we could first model the average optimal travel distance without road network, and then calibrate the free parameters in the same formula.

Following Ref. (*17*), in which the authors assume the residents find the nearest facility in terms of the Euclidian distance, the total travel distance in one *service community* can be write as $p_j^S \cdot g_j^S \cdot (a_j^S)^{0.5}$, then we can calculate the average travel distance of all population in the city as follows:

$$L = \frac{1}{P} \cdot \sum_{j=1}^{N} g_j^S p_j^S (a_j^S)^{0.5} \quad , \tag{1}$$

where P is the total population in the city, N is the number of facilities or *service communities*, p_j^S is the population in the *service community* of the jth facility, a_j^S denotes the total area of blocks in the community..

In this work, we assume the residents in the blocks with facilities have constant travel distance, l_{min} which is close to 0.5 km near the Equator. Consequently, we could separate the Eq. 1 into two terms, for population in the blocks with and without facilities:

$$L = \frac{1}{P} \cdot \left(l_{min} \cdot \sum_{j=1}^{N} p_j + \sum_{j=1}^{N} g_j^S \tilde{p}_j^S (a_j^S)^{0.5} \right) \quad , \tag{2}$$

where $\tilde{p}_j^S$ denotes the population in the *service community* of jth facility after removing the block where the facility j is located, that is $\tilde{p}_j^S = p_j^S - p_j$. We then simplify Eq. 2 by defining $p(N) = \frac{1}{P}\sum_{j=1}^{N} p_j$ as the share of the population in blocks with facilities, and we have

$$L = l_{min} \cdot p(N) + \frac{1}{P} \cdot \sum_{j=1}^{N} g_j^S \tilde{p}_j^S (a_j^S)^{0.5} \quad . \tag{3}$$

The first term in this equation represents the travel distance spent by the population residing in the blocks with facilities and the second one represents the travel distance of the population in the blocks without facilities. The travel distance of $p(N)$ in the first term is assigned to be l_{min}, which is assumed to be 0.5 km in our experiments, and thus, it is considerable only for the case of a large number of facilities. For small values of N, the second term determines the value of L. In this regime, the continuous block density assumption in Ref. (*17*) is not valid as there can be large empty patches in the *service community*. For this regime, when the second term dominates the value of L, we should consider the populated area inside the *service community* instead of the total area. Thus, instead of a_j^S we define $a_{j,occ}^S \approx n_{j,occ}^S \cdot \bar{a}$, where $n_{j,occ}^S$ denotes the number of blocks with population above a threshold within the *service community*. The threshold is set to 500 in real cities, which is a commonly used threshold to distinguish urban from rural regions. Thus, when N is small, it is more feasible to rewrite the second term in Eq. 3 as,

$$\frac{1}{P} \cdot \sum_{j=1}^{N} g_j^S \tilde{p}_j^S (a_{j,occ}^S)^{0.5} \quad . \tag{4}$$

Next, we define D_{occ} as the ratio between the number of facilities to assign N and the number of occupied blocks in the city N_{occ}, that is, $D_{occ} = N/N_{occ}$. In Fig. S5A, we show the number of occupied blocks $n_{j,occ}^S$ versus the total number of blocks n_j^S in *service communities* when the facilities are optimally distributed under varying D_{occ}. We fit the relation with power law $n_{j,occ}^S \propto (n_j^S)^\gamma$ on all values of D_{occ} for each city and find good fitting except for Paris. Indeed, Paris is much larger than other cities in our experiments and the exiting of many depopulated zones causes the failure of power law fitting. The γ is always less than 1.0, indicating that the fraction of occupied blocks in *service communities* increases sublinearly with the area of communities.

In the following equations, we rewrite n_j^S and $n_{j,occ}^S$ with the total area a_j^S and populated area $a_{j,occ}^S$, respectively.

$$\begin{aligned} n_{j,occ}^S &\propto (n_j^S)^\gamma \\ (\bar{a})^\gamma \cdot n_{i,occ}^S &\propto (\bar{a})^\gamma \cdot (n_j^S)^\gamma \\ (\bar{a})^{\gamma-1} \cdot \left(\bar{a} \cdot n_{j,occ}^S\right) &\propto \left(\bar{a} \cdot n_j^S\right)^\gamma \\ (\bar{a})^{\gamma-1} \cdot a_{j,occ}^S &\propto (a_j^S)^\gamma \\ a_{j,occ}^S &\propto (\bar{a})^{1-\gamma} \cdot (a_j^S)^\gamma \end{aligned} \tag{5}$$

As both of the average block area $\bar{a}$ and γ are constant in one city, we could find the power law relation between the populated area $a_{j,occ}^S$ and the total area a_j^S in the *service communities* with the same exponent in each city, that is, $a_{j,occ}^S \propto (a_j^S)^\gamma$. Thus, Eq. 4 can be rewritten as:

$$\frac{1}{P} \cdot \sum_{j=1}^{N} g_j^S \tilde{p}_j^S (a_j^S)^{0.5\gamma} \tag{6}$$

For simplification, we make the following assumptions: (i) the geometric factor g_j^S in each *service community* is a constant value for a given city, that is $g_j^S \approx g_{city}$. The same assumption is made in Ref. (*17*). (ii) the service area of each community a_j^S can be taken out from the summation by introducing an average service area $\overline{a^S}$ for one city, and we have $\overline{a^S} = \bar{a} \cdot N_{max}/N$. Then Eq. 6 can be approximated by:

$$\begin{aligned} & \frac{1}{P} \cdot g_{city} \cdot (\overline{a^S})^{0.5\gamma} \cdot \sum_{j=1}^{N} \tilde{p}_j^S \\ = \quad & \frac{1}{P} \cdot g_{city} \cdot \left(\bar{a}\frac{N_{max}}{N}\right)^{0.5\gamma} \cdot \sum_{j=1}^{N} \tilde{p}_j^S \\ = \quad & \left(g_{city} \cdot (\bar{a}N_{max})^{0.5\gamma}\right) \cdot N^{-0.5\gamma} \cdot \left(\frac{1}{P}\sum_{j=1}^{N} \tilde{p}_j^S\right) \end{aligned} \tag{7}$$

In the first component of this equation, the geometric factor g_{city}, the average block area $\bar{a}$, and the number of blocks N_{max} are all constant for each city. Moreover, from the previous text, we find γ, as the exponent of power low between $\langle n^S_{j,occ} \rangle$ and $\langle n^S_j \rangle$, is also constant for a given city, as shown in Fig. S5A. Therefore, we could use one single variable A to replace the first component in Eq. 7. For the third component, $\sum_{j=1}^{N} \tilde{p}^S_j / P$ denotes the share of population in the blocks without facilities in the city and equals to $1 - p(N)$. Then we can simplify Eq. 4 to

$$A \cdot N^{-0.5\gamma} \cdot (1 - p(N)) \tag{8}$$

where

$$A = g_{city} \cdot (\bar{a} N_{max})^{0.5\gamma} \tag{9}$$

We further replace 0.5γ with λ, then we finally rewrite Eq. 3 as:

$$L(N) = l_{min} \cdot p(N) + A \cdot N^{-\lambda} \cdot (1 - p(N)) \tag{10}$$

Since λ relates the populated and total areas, we interpret it as a clumping exponent describing the spatial dispersion pattern of the population in cities. The factor $AN^{-\lambda}$ represents the average travel distance of population in blocks without facilities.

Note that, so far, at no step have we used the fact that the localization of facilities is optimizing the travel distance, but only that there is a power law relation between $\langle n^S_{j,occ} \rangle$ and $\langle n^S_j \rangle$. In principle, this equation should work for various assignment strategies of facilities. To further understand it, we next discuss the functional form of $1 - p(N)$, the share of population in the blocks without facilities.

S4.2 On the functional form of population in blocks without facilities

In Fig. S5B, we show $1 - p(N)$ as a function of N for our 12 cities on the log-linear plots in the descending order in terms of their UCI values. As the share of population in blocks without facilities $1 - p(N)$ dominates the average travel distance L in Eq. 10 when N is small, we focus on the behavior of $1 - p(N)$ for N in a limit range. According to their behavior shown in Fig. S5B, we can classify the cities into two groups, monocentric and polycentric cities. For monocentric cities, comprised by Paris, Dubai, Barcelona, Riyadh, Doha, Boston, and NYC, $1 - p(N)$ follows a clear exponential decay, i.e. $1 - p(N) = e^{-\alpha \cdot N}$, for N in a limit range. For the polycentric ones, made up by the remaining cities, LA, London, Mexico City, Dublin, and Melbourne, we find the decay is slower than an exponential but faster than a linear one, by observing that the markers are above the line when N is small. The linear case corresponds to the natural limit, a perfectly homogeneous city where $p(N)$ increases linearly with N. Note that this classification is consistent with the urban centrality index UCI, monocentric cities correspond to the highest values of UCI.

Coming back to the Eq. 10, the functional form of $p(N)$ is only crucial for scenarios with a large number of facilities, when the first term starts controlling the value of the travel distance. For most of the region of interest, from few to an intermediate number of facilities, the Eq. 10 does not demand the use of an accurate expression for $1 - p(N)$. Fig. S6B shows how, even for the polycentric cities, an exponential form for $1 - p(N)$ gives a good description of the average travel distance when we fit it using the Eq. 10. Thus, we decided to use this functional form in the main text.

We thus recall the standard urban models for describing monocentric cities (*57-61*) assume a negative exponential density pattern $\rho = \rho_0 \cdot e^{-\delta \cdot r}$, where r is the distance to the densely populated city center and δ is the gradient at which the density changes. Thus, if the final spatial distribution is a sample of blocks weighted by the population and, population in cities are spatially clustered, it results naturally to obtain an exponential decay. Consistently, the density patterns of sprawled cities do not match with this monocentric description. Hence, an extensional work of our results should be to find the relationship between our exponent α and the density gradient δ from the urban models.

S4.3 Simple model of travel distance with number of facilities

In the previous Note S4.1, we modeled the average travel distance L with the number of facilities to assign N and the share of population in the N blocks with facilities $p(N)$ in Eq. 10. In Note S4.2, we discussed the relation between the share of population in the blocks without facilities $1-p(N)$ with the number of facilities N and found an exponential decay when N is limited. Also in our experiments, we set the travel distance within blocks as a constant value, 0.5 km. Therefore, we can simply model the average travel distance in *optimal* scenario with

$$L(N) = 0.5 \cdot \left(1 - e^{-\alpha N}\right) + A \cdot N^{-\lambda} \cdot e^{-\alpha N} \quad , \tag{11}$$

where the number of facilities to assign, N, is the only one variable to input; the decay exponent α is derived via fitting $1-p(N)$ using N in each city, see Fig. S5B. The other two parameters λ and A are treated as free parameters and they are calibrated with the simulated L with varying N in each city.

In reality, the facility planning with limited resources (small N) is much more important than the planning with plenty of resources. Therefore, the assumption that $1-p(N)$ follows an exponential decay with N makes our model work better when resources to assign are limited. Besides, as can be seen from Fig. S5B, the exponential function $1 - p(N) = \exp(-\alpha \cdot N)$ can fit better in monocentric cities than policentric ones, indicating that our simple model in Eq. 11 performs better in monocentric cities. As we leave both A and λ as free parameters that are calibrated using the simulation results, the exponential models of polycentric cities can also be well fitted. The simulation results and fitted models for 17 toy cities and 12 real cities are presented in Figs. S6A and S6B, respectively. The fitted parameters are presented in Table S2. For the most monocentric toy cities for which UCI scores are above 0.9, the model can not fit the simulation well as only a small number of blocks are occupied by population in these toy cities, resulting in an unreliable estimation of α. In reality, almost all cities have UCI lower than 0.8.

S4.4 Towards a universal model of travel distance

Note that the $L(N)$ curves for different cities are strikingly similar. This similarity stems from the near-universal values of the exponent λ (see Table S2), explaining the similar power-law decays for not too high values of N. We thus assume λ as universal and use the average value $\overline{\lambda}$=0.382 for all cities. This result suggests that $L(N)$ might also be universal. Scaling arguments could help in giving us a deeper understanding of the parameters in Eq. 11, and thus revealing a unified expression explaining all the cities.

The most direct interpretation of the parameter α in the negative exponential can be made by taking the derivative of $g(N) = 1 - p(N) = e^{-\alpha N}$. Then

$$\frac{dg(N)}{dN} = -\alpha e^{-\alpha N} = -\alpha g(N) \tag{12}$$

and thus

$$\frac{dg(N)}{g(N)} = -\alpha dN \rightarrow \frac{\Delta g}{g(N)} = -\alpha \quad , \tag{13}$$

where we have used the fact that N is a discrete variable, i.e. dN=ΔN=1. This equation implies that α is the percentage change in population share in blocks without facilities when the number of facilities is increased by one. One can expect that α is proportional to the average share of population per block and thus it should vary inversely proportional to the number of blocks in the city. Figs. S7A and S7B show that $\alpha \sim 1/N_{max}$ with Paris as an outlier. Going further, since $A \sim g_{city}\overline{a}^{\overline{\lambda}} N_{max}^{\overline{\lambda}}$ (see Eq. 7 and Eq. 10), we can expect that $A \propto \alpha^{-\overline{\lambda}}$. Fig. S7C confirms this, $A = 1.4443\alpha^{-\overline{\lambda}}$. Thus far, we can rewrite Eq. 11 as follows:

$$L(N) = 0.5 \cdot \left(1 - e^{-\alpha N}\right) + 1.4443 \cdot (\alpha N)^{-\overline{\lambda}} \cdot e^{-\alpha N} \quad . \tag{14}$$

In the main text, Fig. 5F tests for universality in the $L(N)$ curves. Using the α for each city, we plot L vs. αN which removes the city-dependent term from Eq. 14. With no other adjustments, the resulting curves nearly coincide, as if collapsing on a single, universal curve.

It would be useful to have a simple and accurate way to estimate α. Let's retake the fact that $\alpha \sim 1/N_{\max}$. The reason Paris is an outlier is that population is unevenly distributed across the total surface, meaning it has many empty or almost empty blocks (parks, natural reserves or rural lands). From the optimization algorithm perspective, those blocks are not attractive for putting a facility inside. Thus, N_{occ} could better explain the values for α. Fig. S7D shows that, in a very good a agreement, $\alpha \approx 1.833/N_{occ}$.

S4.5 Number of facilities *N* vs accessibility *L*

From the perspective of application, it would be interesting to estimate the number of facilities needed to reach a given accessibility value L, i.e. we want to solve the transcendental Eq. 14. To do so, note that (1) the first term only takes small values from 0 to 0.5 and (2) the second term allows to invert the function. Thus, we wonder for the regimes where the accessibility $L(N)$ can be approximated by only the second term

$$L(N) \approx 1.4443(\alpha N)^{-\overline{\lambda}} e^{-\alpha N} \quad . \tag{15}$$

Note that this functional form displays a transition from a power-law to an exponential decay. Thus, a reasonable criterion is to find the point where the function starts becoming an exponential decay. Deriving equation

$$\frac{dL(N)}{dN} \approx L(N) \left(-\frac{\overline{\lambda}}{N} - \alpha \right) \quad , \tag{16}$$

we can see that the critical point occurs when the two factors in parenthesis are comparable, i.e. $N = \overline{\lambda}/\alpha$. From that point, the exponential parameter α controls the decay. Fig. S7E gives a visual prove of this, using the α values for Paris and Dublin as examples. As a result, for $0 < N < \overline{\lambda}/\alpha$ or L>1.42 km (replacing N by $\overline{\lambda}/\alpha$ in Eq. 15), the approximation performs reasonably well and, the inverse function for N is

$$N(L;\alpha) \approx \frac{\overline{\lambda}}{\alpha} W\left(\frac{(L/1.4443)^{-1/\overline{\lambda}}}{\overline{\lambda}}\right) \quad , \tag{17}$$

where $W(\cdot)$ is the ProductLog or Lamber-W function and $\overline{\lambda}$ is a constant given above. Fig. S8 here and Fig. 5H in the main text show Eq. 17 gives a fair prediction for N. The application of this result to other cities is straightforward. Once the anticipated accessibility is defined, one can calculate α using the fact that $\alpha \sim 1.833/N_{occ}$, and thus can use Eq. 17 to estimate the number of facilities N needed to accomplish the desired accessibility.

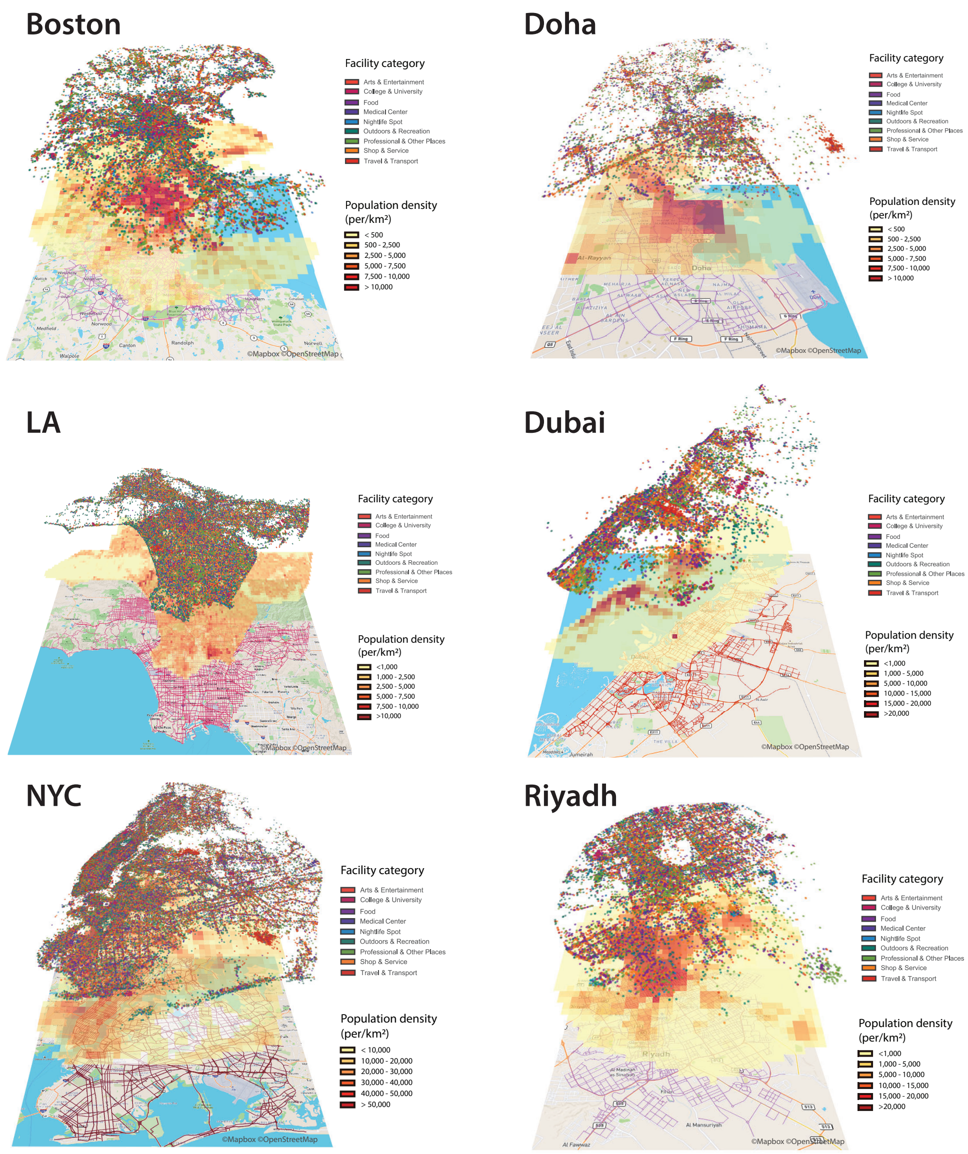

Fig. S1. Road network, population density, and the facilities in each category in the six cities. All facilities from Foursquare are grouped into 9 categories, as shown in the legend.

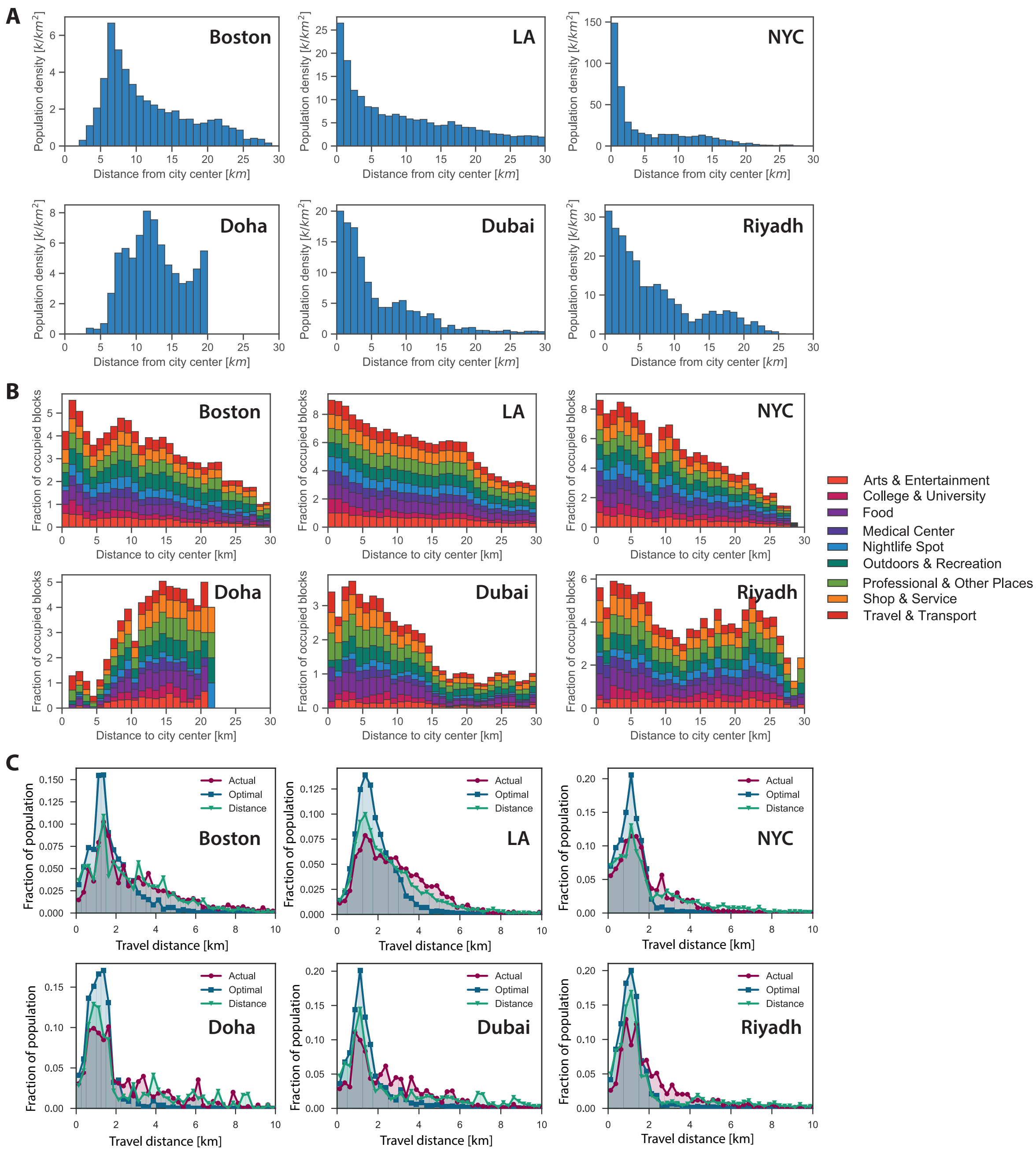

Fig. S2. Distribution of population, facilities, and travel distance in the six cities. (**A**) Distribution of population within varying distance to the city center. (**B**) Distribution of different categories of facilities within varying distance to the city center. To achieve this plot, the same type of facilities in the same block are first merged into one. Then we count the number of facilities per category per block. There are 9 categories of facilities in the Foursquare datasets. The population of Boston and Doha have similar distribution within 15 km where less residents reside in the city center, while residents are congregated near city centers in the other cities. The facilities in Boston, LA, NYC, and Dubai are congregated near city centers, while the facilities in Doha, and Riyadh are distributed more uniformly. (**C**) Comparison of the distribution of travel distance to hospital between the actual scenario, the optimal scenario, and the distance based optimal (distance) scenario used in Ref. (*18*) and (*19*). In the distance scenario, the Voronoi cell around each facility is used as a proxy of the tendency of individuals to selecting the closest facility. For all of the three scenarios, once the locations of facilities are confirmed, the travel distance is calculated in the road network from the place of each residence to the nearest facility. Optimal scenario always produces short travel distance for large proportion of population. The performance of distance scenario is approximated to the actual, indicating the distance based optimization is far from the optimal in terms of travel distance in road network.

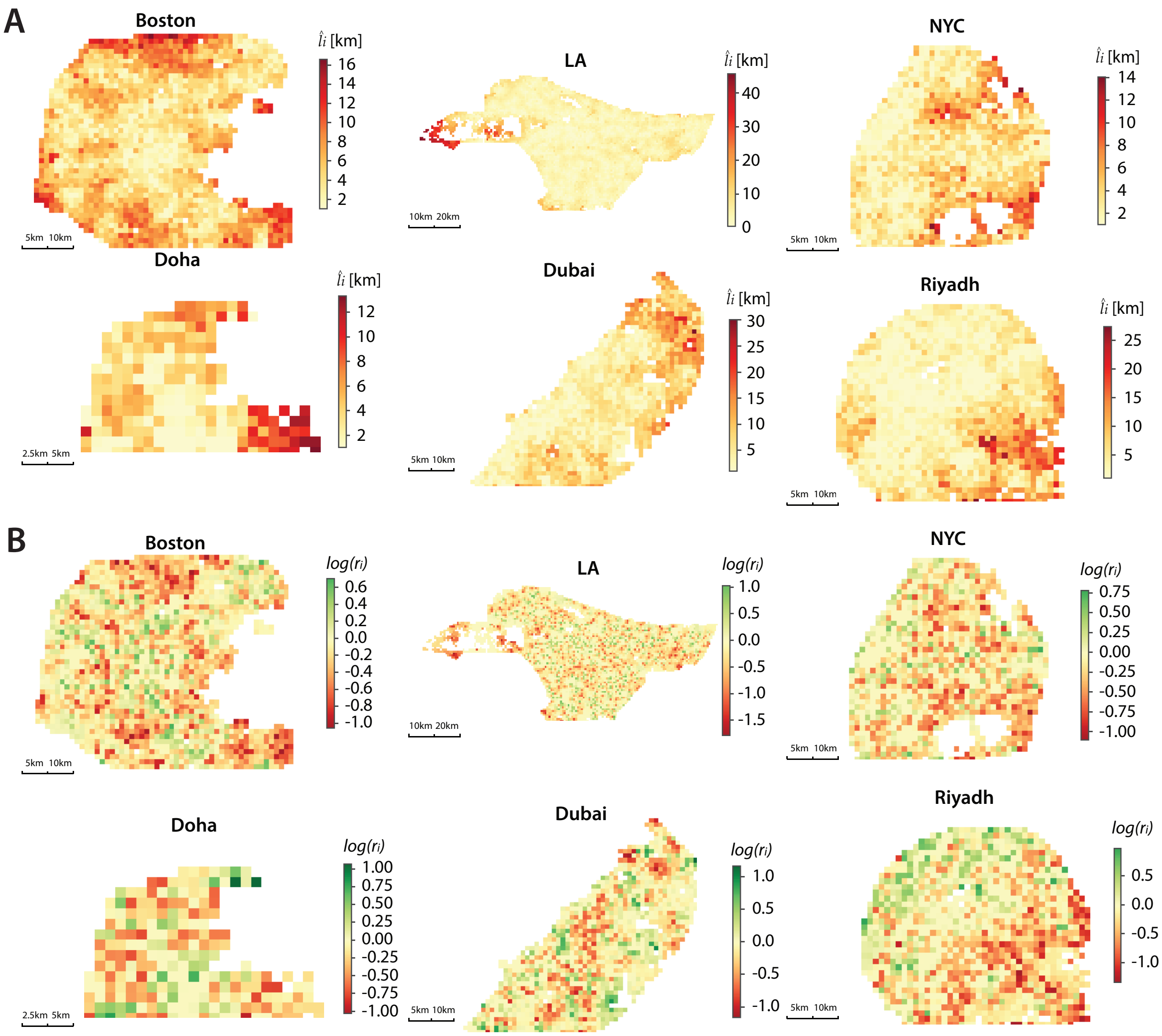

Fig. S3. Actual travel distance and gain index to hospitals of each block. (**A**) Actual travel distance to hospitals $\hat{t}_i$ of each block in the six cities. (**B**) Gain index r_i of each block in the six cities. The populated blocks always have shorter travel distance and larger gain index than the depopulated ones once the hospitals are redistributed optimally. The reason is that in reality, some hospital are located in region with low population density and increase the average travel distance of population in the *service communities*.

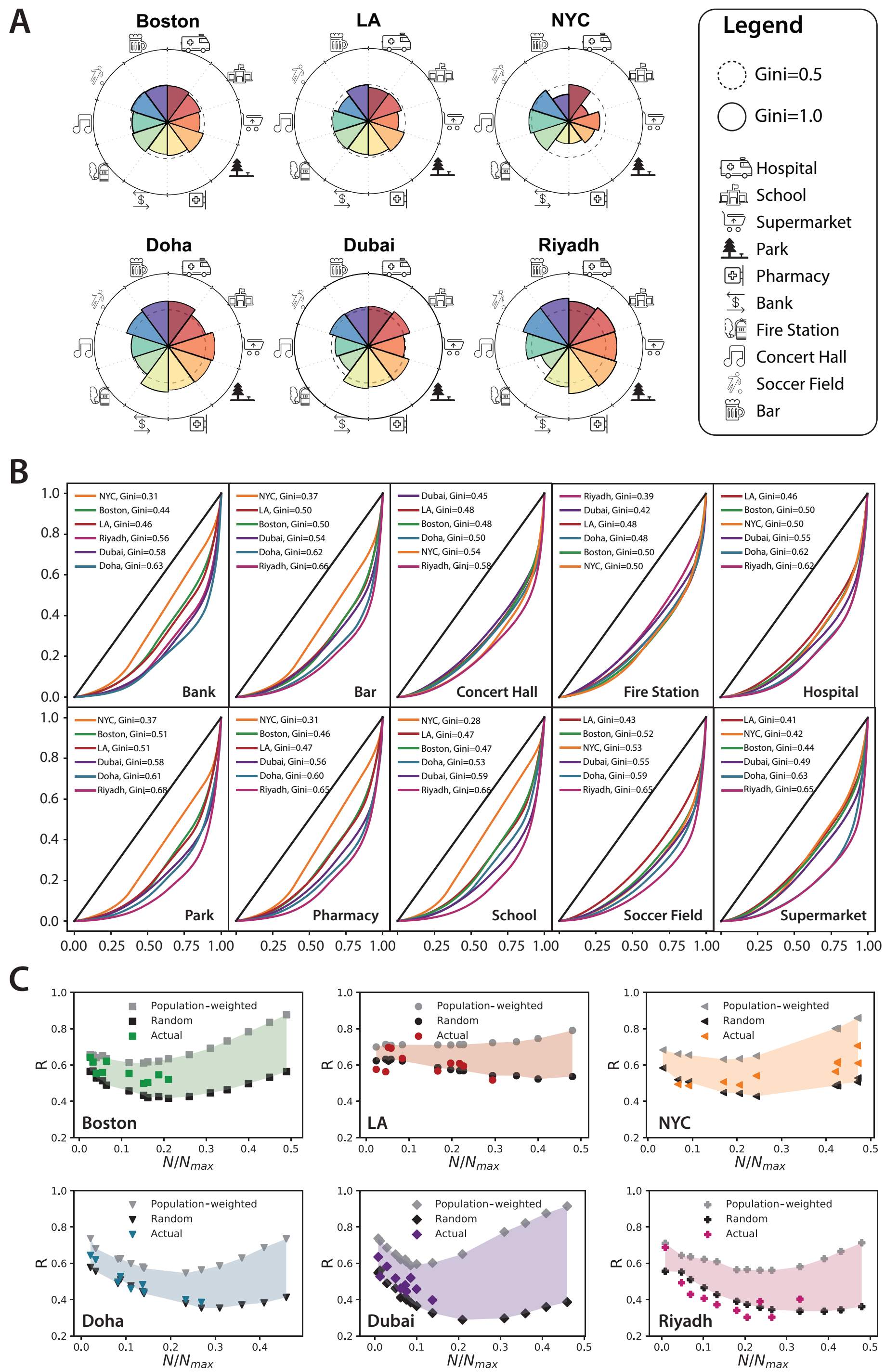

Fig. S4. Gini coefficient of the block gain index and optimality index per facility type per

city. (**A**) Gini coefficient of the block gain index per facility type per city. A Gini coefficient of zero indicates perfect equality, where all blocks have the same gain index. The closer the Gini coefficient is to 1, the less equitable the distribution of facilities. The solid line refers to 1, representing maximum inequality and the dashed line refers to 0.5. The Gini coefficient of different facility types are similar in Boston. NYC shows evidently lower Gini than other cities on schools, parks, pharmacies, banks, and bars. Overall, the facilities in GCC cities are planned more unequally than U.S. cities except the fire stations. (**B**) Lorenz curves by city and type of facility. The facility types are sorted in the alphabet order. In the legend of each panel, cities are sorted by Gini coefficient in increasing order. Among the 10 types of facilities, the three U.S. cities (Boston, LA, NYC) have more equal distribution than Gulf Cooperation Countries cities (Doha, Dubai, Riyadh) except concert halls and fire stations, mainly due to the larger density of facilities. NYC has the best equality in banks, bars, parks, pharmacies and schools. LA has the best equality in hospital, soccer field and supermarket. The facility planning in Riyadh is the most unequal. It has the most inequality in 8 of the 10 types of facilities, except banks and fire stations. (**C**) Optimality index R for actual distribution of facilities and the two extreme strategies of facility assignment methods, *random* and *population-weighted*. The dark and light gray markers represent the R of the *random* and *population-weighted* assignment strategy, respectively. The colored markers represent the R of the actual distribution of 10 types of facilities. Each point in the simulated assignments corresponds to the average over 10 runs.

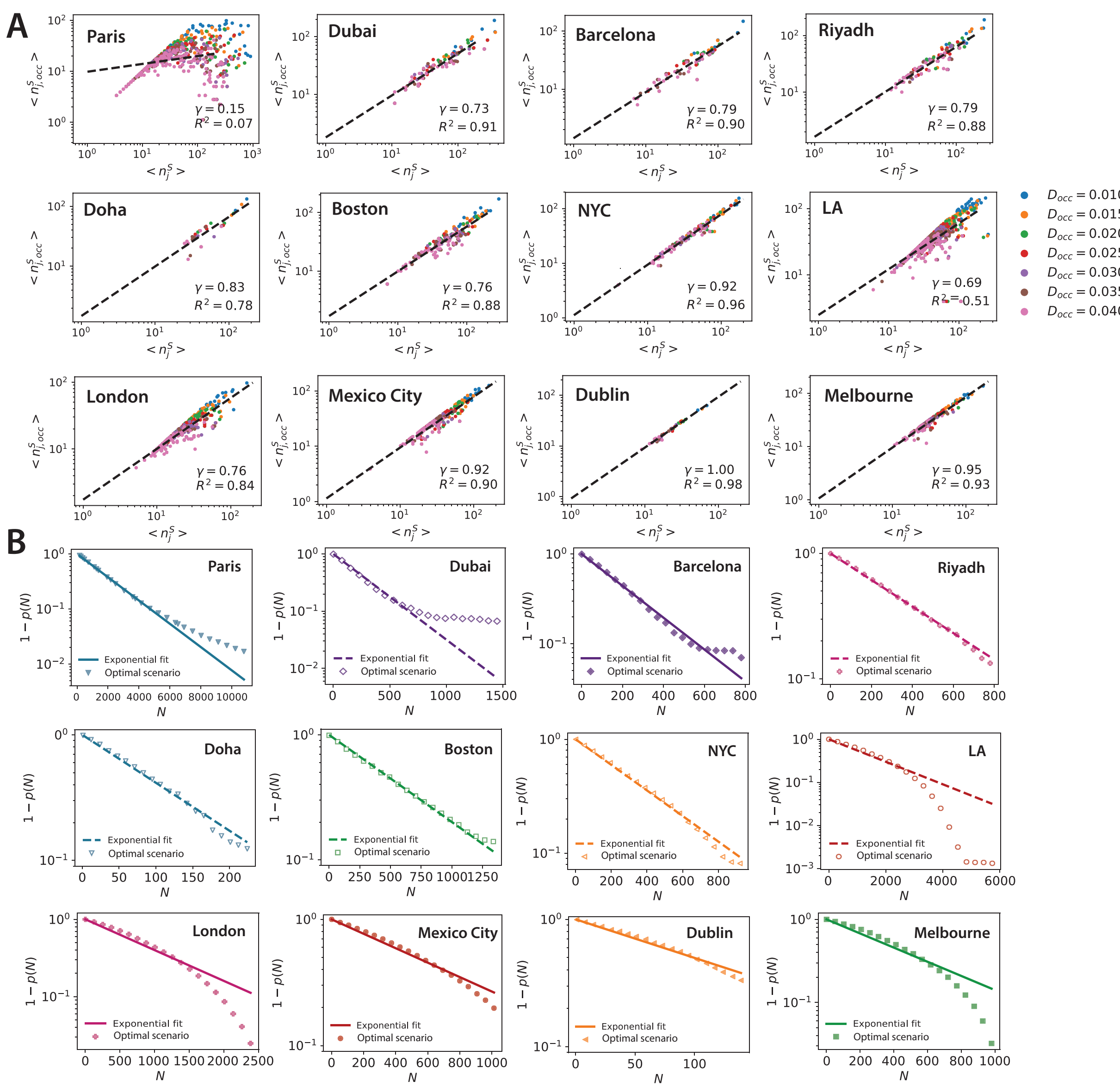

Fig. S5. Fitting the number of occupied blocks and the share of population in blocks without facilities. (**A**) Relation between the number of occupied blocks $\langle n^S_{j,occ} \rangle$ and the number of blocks $\langle n^S_j \rangle$ in *service communities* for varying D_{occ} on a log-log plot. The cities are ranked by UCI in the descending order. The values of UCI are given in Table S2. For a given D_{occ} in a city, we first find the number of facilities to assign, N, then we find their optimal locations by the optimization algorithm, popstar (*50*). Next we count the n^S_j and $n^S_{j,occ}$ in each service community of facility. Each colored point represents a *service community*. We fit the relation between $\langle n^S_{j,occ} \rangle$ and $\langle n^S_j \rangle$ with power law, that is $n^S_{j,occ} \propto (n^S_j)^\gamma$. The dashed line displays the fitted power law and the exponent γ is always less than 1 for all cities. The power law can fit the relation well for the cities with large R^2 except Paris. Paris is the largest city in area in our experiments and the exiting of many depopulated zones causes the failure of power law fitting. (**B**) Fitting the relation between the share of population in blocks without facilities, $1 - p(N)$, and the number of facilities, N, on a log-linear plot. The cities are ranked by UCI in the descending order. The markers in the plots represent the results from the *optimal* scenarios. For each value of N, we first find their optimal locations, then count the population in the blocks without facilities at city scale. The relation between $1 - p(N)$ and N is fitted with exponential function, $1 - p(N) = e^{-\alpha \cdot N}$. The solid or dashed lines represent the fitted exponential function. The fitted value of α for each city is presented in Table. S2.

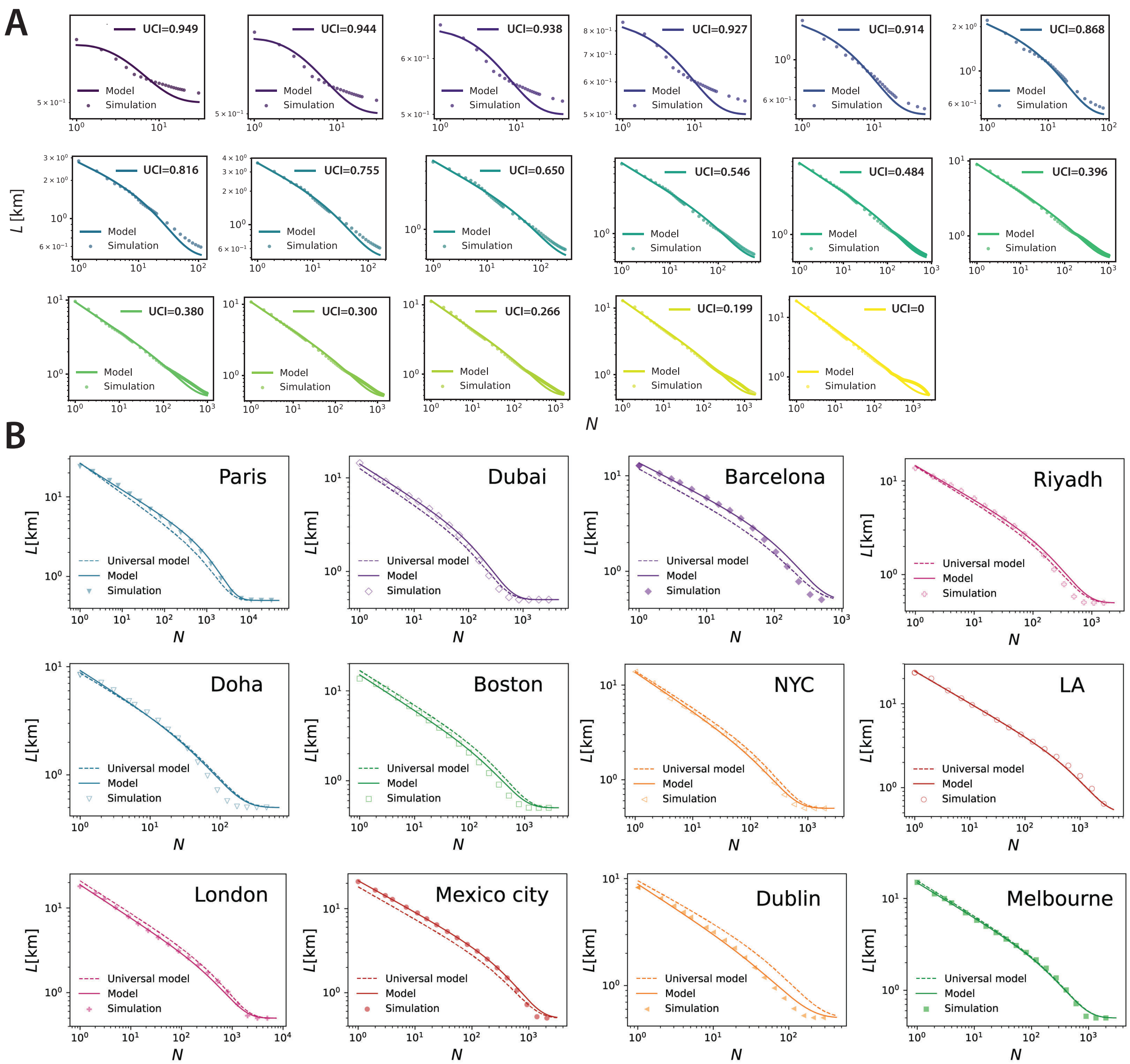

Fig. S6. The modeled and simulated average travel distance in *optimal* scenario in toy and real-world cities. (**A**) The modeled and simulated average travel distance in *optimal* scenario L versus the number of facilities N in the 17 toy cities. The cities are ranked by UCI in the descending order. The markers represents the simulated average travel distance given the number of facilities. The solid lines represent the fitted exponential function $L(N) = 0.5 \cdot (1 - e^{-\alpha N}) + A \cdot N^{-\lambda} \cdot e^{-\alpha N}$. The fitted parameters and UCI of each city are shown in Table S2. (**B**) The modeled and simulated average travel distance in *optimal* scenario L versus the number of facilities N in the 12 real cities. The cities are ranked by UCI in the descending order. The markers represents the simulated average travel distance given the number of facilities. The solid or dashed lines represent the fitted exponential function $L(N) = 0.5 \cdot (1 - e^{-\alpha N}) + A \cdot N^{-\lambda} \cdot e^{-\alpha N}$. The fitted parameters and UCI of each city are shown in Table S2.

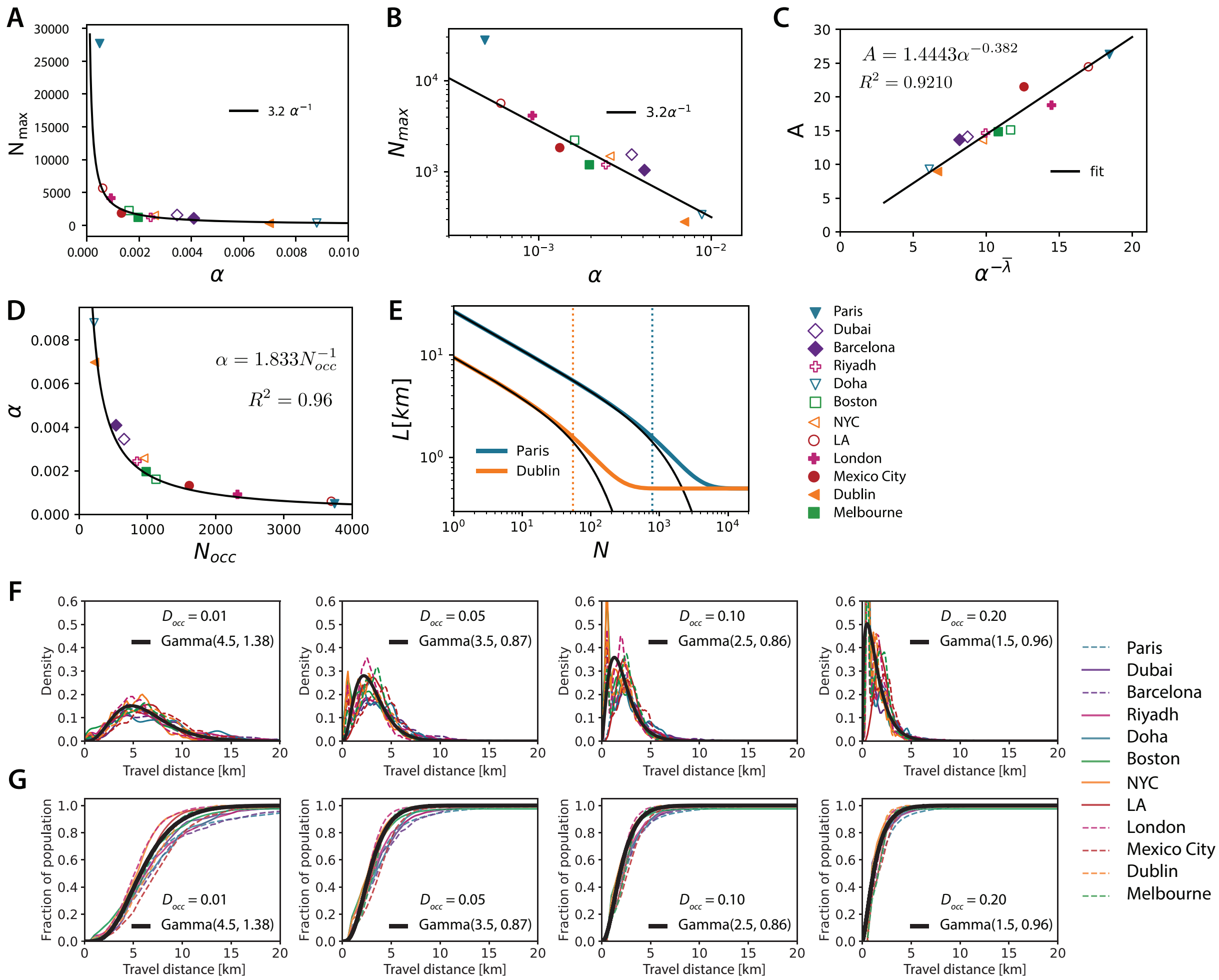

Fig. S7. Simple model of travel distance with number of facilities. (**A**)-(**B**) The total number of blocks $N_{\max}$ is approximately inversely proportional to the parameter α, with Paris as a clear outlier. (**C**) Linear relationship between constant A (Eq. 11) and $\alpha^{-\overline{\lambda}}$, with the average $\overline{\lambda} = 0.382$. (**D**) Relationship between the exponent α and the number of occupied blocks N_{occ}. (**E**) Black solide lines are $L(N)$ curves approximated by the second term of the Eq. 14, i.e. $L(N)$=$1.4443(\alpha N)^{-\overline{\lambda}}e^{-\alpha N}$ (black solid lines). Colored full lines correspond to the complete expression for $L(N)$. Vertical dotted lines mark the limit of the reliability of the approximation, i.e. N=$\overline{\lambda}/\alpha$. The curves are obtained using the α values for Dublin and Paris. (**F**) Distribution of personal travel distance from their resident blocks to the nearest facilities when the facilities are optimally distributed under $D_{occc} = 0.01,\ 0.05,\ 0.1,\ 0.2$, respectively. The distribution of travel distance clearly follows a Gamma distribution, $G(x;\kappa,\theta) = \frac{1}{\Gamma(\kappa)\theta^{\kappa}} x^{\kappa-1} e^{-x/\kappa}$, in which the mean value $\mu = \kappa\theta$, κ and θ control the shape and scale of the gamma distribution, respectively. The travel distance distributions for different cities with fixed D_{occ} display similar tendency and can be matched with the gamma distributions. For each selected value of D_{occ}, the mean value of gamma distribution, μ, equals to the average optimal travel distance, L, and the shape κ is manually selected to achieve a good fit. The Gamma distribution is shown with the black solid curve. To achieve a uniform gamma distribution among all cities, we calculate the collapsed $L(D_{occ})$ with the same set of parameters $\{\alpha = 2.0, A = 1.0, \lambda = 0.4\}$, that is, $L(D_{occ}) = 0.5 \cdot (1 - e^{-2.0D_{occ}}) + 1.0 \cdot D_{occ}^{-0.4} \cdot e^{-2.0D_{occ}}$. (**G**) CDF of the travel distance and the selected Gamma distribution when the facilities are optimally distributed under $D_{occ} = 0.01,\ 0.05,\ 0.1,\ 0.2$ respectively. The CDF of travel distance in different cities show clear collapses, especially for large D_{occ}. The black solid curve shows the CDF of the Gamma distribution.

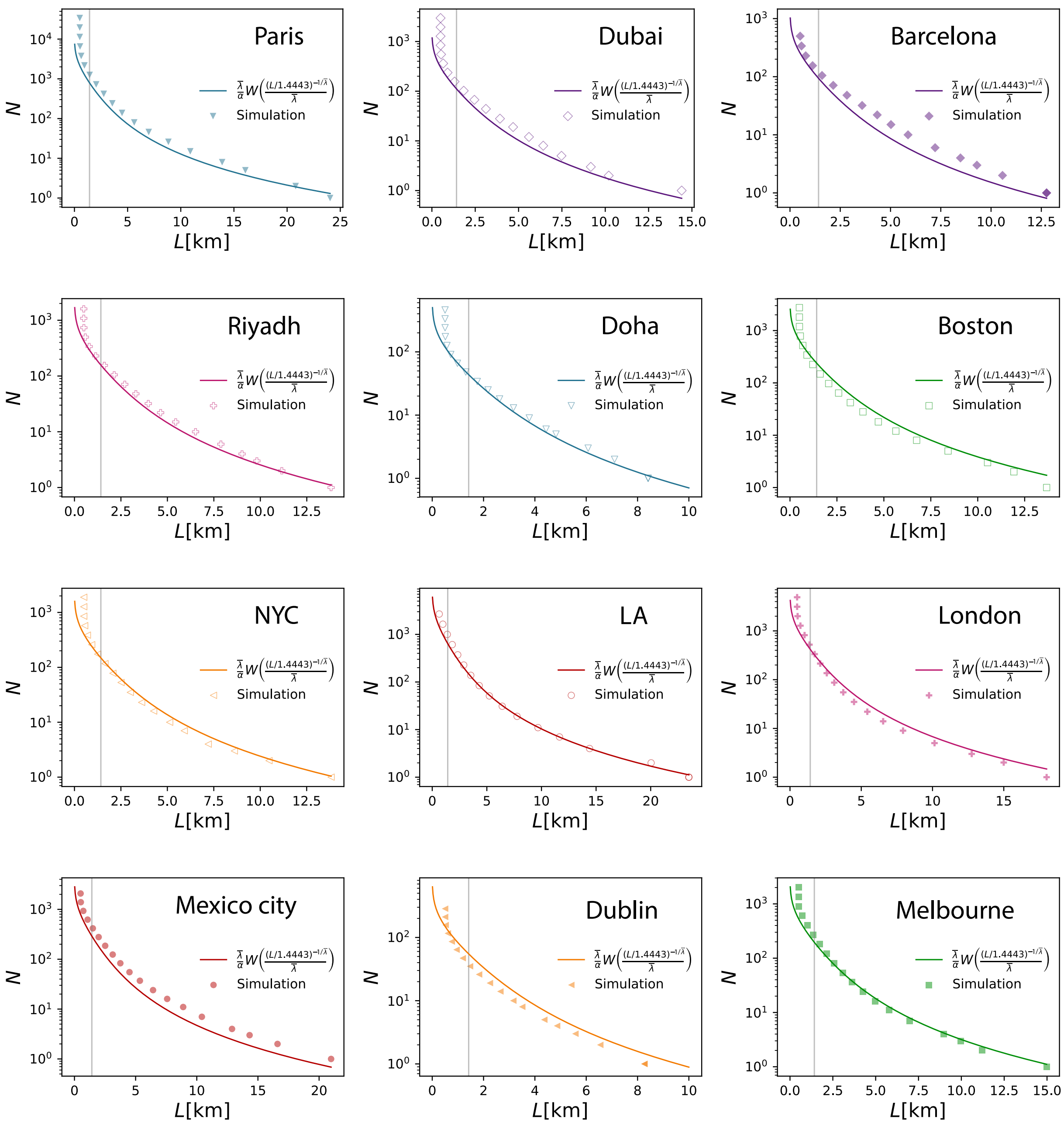

Fig. S8. Comparison between the simulation results and the universal function. The approximations of N are obtained with $N(\overline{\lambda}, \alpha; L)$, Eq.17. For $L > 1.42$ km (gray vertical lines), the approximation performs reasonable well for all the cities.

Table S1: **Best fitted exponent of the power law for the actual and optimal distribution of facilities.** The exponents are inconsistent in the actual scenario due to deliberate planning. The exponents in the optimal scenario are generally near 2/3 except some high density facilities in NYC.

	Facility	Boston	LA	NYC	Doha	Dubai	Riyadh
Actual scenario	Hospital	0.78	0.98	0.50	0.93	0.44	0.30
	School	0.54	0.60	0.29	0.23	0.09	0.19
	Supermarket	0.37	0.63	0.45	-0.19	0.43	0.05
	Park	0.56	0.28	0.22	0.03	0.50	0.18
	Pharmacy	0.64	0.84	0.34	0.40	0.34	0.12
	Bank	0.48	0.65	0.29	0.48	0.35	0.23
	Fire Station	0.69	0.28	0.27	0.81	0.07	0.20
	Concert Hall	1.12	1.14	0.58	0.24	0.92	0.00
	Soccer Field	0.25	0.37	0.52	0.08	0.16	-0.41
	Bar	0.64	0.74	0.26	0.33	0.65	0.04
Optimal scenario	Hospital	0.70	0.72	0.65	0.64	0.74	0.60
	School	0.58	0.76	0.23	0.59	0.80	0.62
	Supermarket	0.70	0.66	0.52	0.58	0.80	0.75
	Park	0.50	0.72	0.22	0.71	0.80	0.65
	Pharmacy	0.64	0.56	0.28	0.71	0.67	0.58
	Bank	0.56	0.78	0.28	0.52	0.64	0.48
	Fire Station	0.70	0.64	0.60	0.40	0.79	0.41
	Concert Hall	0.64	0.69	0.72	0.57	0.84	0.61
	Soccer Field	0.71	0.67	0.72	0.64	0.75	0.65
	Bar	0.60	0.78	0.29	0.67	0.87	0.68

Table S2: **Fitted parameters of the 17 toy cities and the 12 real cities.** We first fit the share of population in the blocks without facilities $1 - p(N)$ with α, then calibrate the A and λ with the simulated travel distance via $L(N) = 0.5 \cdot (1 - e^{-\alpha N}) + A \cdot N^{-\lambda} \cdot e^{-\alpha N}$.

	N_{max}	N_{occ}	UCI	α	A	λ
Toy cities	$10,000$	32	0.949	1.92×10^{-1}	0.537	-0.013
	$10,000$	32	0.944	1.78×10^{-1}	0.573	-0.019
	$10,000$	44	0.938	1.50×10^{-1}	0.680	-0.017
	$10,000$	52	0.927	1.23×10^{-1}	0.856	0.007
	$10,000$	52	0.914	1.21×10^{-1}	1.673	0.066
	$10,000$	87	0.868	5.34×10^{-2}	2.173	0.144
	$10,000$	119	0.816	3.27×10^{-2}	2.837	0.200
	$10,000$	170	0.755	1.76×10^{-2}	3.675	0.260
	$10,000$	284	0.650	7.86×10^{-3}	5.175	0.308
	$10,000$	551	0.546	4.05×10^{-3}	6.732	0.336
	$10,000$	740	0.484	3.09×10^{-3}	7.677	0.351
	$10,000$	$1,026$	0.396	2.22×10^{-3}	9.118	0.371
	$10,000$	984	0.380	2.26×10^{-3}	9.427	0.394
	$10,000$	$1,361$	0.300	1.70×10^{-3}	10.736	0.396
	$10,000$	$1,521$	0.266	1.56×10^{-3}	11.381	0.406
	$10,000$	$1,802$	0.199	1.25×10^{-3}	12.972	0.421
	$10,000$	$2,500$	0.000	6.55×10^{-4}	19.161	0.477
Paris	$21,576$	$3,745$	0.500	4.86×10^{-4}	26.31	0.333
Dubai	$1,635$	657	0.351	3.45×10^{-3}	14.09	0.364
Barcelona	$1,022$	539	0.262	4.09×10^{-3}	13.65	0.357
Riyadh	$1,305$	847	0.259	2.44×10^{-3}	14.65	0.360
Doha	380	217	0.240	8.80×10^{-3}	9.29	0.405
Boston	$1,947$	$1,125$	0.212	1.61×10^{-3}	15.11	0.394
NYC	$1,357$	947	0.191	2.58×10^{-3}	13.64	0.409
LA	$5,505$	$3,696$	0.168	6.01×10^{-4}	24.47	0.382
London	$3,071$	$2,320$	0.145	9.16×10^{-4}	18.78	0.390
Mexico City	$2,080$	$1,613$	0.145	1.32×10^{-3}	21.51	0.372
Dublin	285	225	0.101	6.98×10^{-3}	8.937	0.450
Melbourne	$1,148$	981	0.080	1.96×10^{-3}	14.85	0.377

REFERENCES AND NOTES

1. H. A. Makse, S. Havlin, H. E. Stanley, Modelling urban growth patterns. *Nature* **377**, 608–612 (1995).

2. W. Pan, G. Ghoshal, C. Krumme, M. Cebrian, A. Pentland, Urban characteristics attributable to density-driven tie formation. *Nat. Commun.* **4**, 1961 (2013).

3. L. M. Bettencourt, J. Lobo, D. Helbing, C. Kühnert, G. B. West, Growth, innovation, scaling, and the pace of life in cities. *Proc. Natl. Acad. Sci. U.S.A.* **104**, 7301–7306 (2007).

4. L. M. Bettencourt, G. West, A unified theory of urban living. *Nature* **467**, 912–913 (2010).

5. E. Glaeser, Cities, productivity, and quality of life. *Science* **333**, 592–594 (2011).

6. L. M. Bettencourt, The origins of scaling in cities. *Science* **340**, 1438–1441 (2013).

7. D. Weiss, A. Nelson, H. S. Gibson, W. Temperley, S. Peedell, A. Lieber, M. Hancher, E. Poyart, S. Belchior, N. Fullman, B. Mappin, U. Dalrymple, J. Rozier, T. C. D. Lucas, R. E. Howes, L. S. Tusting, S. Y. Kang, E. Cameron, D. Bisanzio, K. E. Battle, S. Bhatt, P. W. Gething, A global map of travel time to cities to assess inequalities in accessibility in 2015. *Nature* **553**, 333–336 (2018).

8. H. D. Rozenfeld, D. Rybski, X. Gabaix, H. A. Makse, The area and population of cities: New insights from a different perspective on cities. *Am. Econ. Rev.* **101**, 2205–2225 (2011).

9. T. Tsekeris, N. Geroliminis, City size, network structure and traffic congestion. *J. Urban Econ.* **76**, 1–14 (2013).

10. L. M. Bettencourt, H. Samaniego, H. Youn, Professional diversity and the productivity of cities. *Sci. Rep.* **4**, 5393 (2015).

11. M. Schläpfer, L. M. A. Bettencourt, S. Grauwin, M. Raschke, R. Claxton, Z. Smoreda, G. B. West, C. Ratti, The scaling of human interactions with city size. *J. R. Soc. Interface* **11**, 20130789 (2014).

12. C. Brelsford, J. Lobo, J. Hand, L. M. A. Bettencourt, Heterogeneity and scale of sustainable development in cities. *Proc. Natl. Acad. Sci. U.S.A.* 8963–8968 (2017).

13. R. Li, L. Dong, J. Zhang, X. Wang, W.-X. Wang, Z. Di, H. E. Stanley, Simple spatial scaling rules behind complex cities. *Nat. Commun.* **8**, 1841 (2017).

14. M. E. Newman, Power laws, Pareto distributions and Zipf's law. *Contemp. Phys.* **46**, 323–351 (2005).

15. J. Depersin, M. Barthelemy, From global scaling to the dynamics of individual cities. *Proc. Natl. Acad. Sci. U.S.A.* **115**, 2317–2322 (2018).

16. M. Barthelemy, The statistical physics of cities. *Nat. Rev. Phys.* **1**, 406–415 (2019).

17. M. T. Gastner, M. Newman, Optimal design of spatial distribution networks. *Phys. Rev. E* **74**, 016117 (2006).

18. J. Um, S.-W. Son, S.-I. Lee, H. Jeong, B. J. Kim, Scaling laws between population and facility densities. *Proc. Natl. Acad. Sci. U.S.A.* **106**, 14236–14240 (2009).

19. K.-W. Tsou, Y.-T. Hung, Y.-L. Chang, An accessibility-based integrated measure of relative spatial equity in urban public facilities. *Cities* **22**, 424–435 (2005).

20. P. Apparicio, A.-M. Séguin, Measuring the accessibility of services and facilities for residents of public housing in Montreal. *Urban Stud.* **43**, 187–211 (2006).

21. S. Macintyre, L. Macdonald, A. Ellaway, Do poorer people have poorer access to local resources and facilities? The distribution of local resources by area deprivation in Glasgow, Scotland. *Soc. Sci. Med.* **67**, 900–914 (2008).

22. H. Dadashpoor, F. Rostami, B. Alizadeh, Is inequality in the distribution of urban facilities inequitable? Exploring a method for identifying spatial inequity in an Iranian city. *Cities* **52**, 159–172 (2016).

23. C. Brelsford, T. Martin, J. Hand, L. M. Bettencourt, Toward cities without slums: Topology and the spatial evolution of neighborhoods. *Sci. Adv.* **4**, eaar4644 (2018).

24. X. Zhou, A. Noulas, C. Mascolo, Z. Zhao, Discovering latent patterns of urban cultural interactions in Wechat for modern city planning, in *Proceedings of the 24th ACM SIGKDD International Conference on Knowledge Discovery & Data Mining* (ACM, New York, U.S.A., 19 to 23 August 2018), pp. 1069–1078.

25. A. N. White, Accessibility and public facility location, *Econ. Geogr* **55**, 18–35 (1979).

26. Z. Tao, Y. Cheng, T. Dai, M. W. Rosenberg, Spatial optimization of residential care facility locations in Beijing, China: Maximum equity in accessibility. *Int. J. Health Geogr.* **13**, 33 (2014).

27. L. E. Olmos, M. S. Tadeo, D. Vlachogiannis, F. Alhasoun, X. Espinet Alegre, C. Ochoa, F. Targa, M. C. González, A data science framework for planning the growth of bicycle infrastructures. *Transp. Res. Part C Emerg. Tech.* **115**, 102640 (2020).

28. H. Samaniego, M. E. Moses, Cities as organisms: Allometric scaling of urban road networks. *J. Transp. Land Use* **1**, 10.5198/jtlu.v1i1.29 (2008).

29. R. Louf, M. Barthelemy, How congestion shapes cities: From mobility patterns to scaling. *Sci. Rep.* **4**, 5561 (2014).

30. T. Louail, M. Lenormand, O. G. Cantu Ros, M. Picornell, R. Herranz, E. Frias-Martinez, J. J. Ramasco, M. Barthelemy, From mobile phone data to the spatial structure of cities. *Sci. Rep.* **4**, 5276 (2014).

31. M. A. Florez, S. Jiang, R. Li, C. H. Mojica, R. A. Rios, M. C. Gonzáles, Measuring the impact of economic well being in commuting networks–A case study of Bogota, Colombia, in *Transportation Research Board 96th Annual Meeting, no. 17-03745* (Washington DC, U.S.A., 8 to 12 January 2017).

32. R. Louf, P. Jensen, M. Barthelemy, Emergence of hierarchy in cost-driven growth of spatial

networks. *Proc. Natl. Acad. Sci. U.S.A.* **110**, 8824–8829 (2013).

33. J. Wang, D. Wei, K. He, H. Gong, P. Wang, Encapsulating urban traffic rhythms into road networks. *Sci. Rep.* **4**, 4141 (2014).
34. S. Çolak, A. Lima, M. C. González, Understanding congested travel in urban areas. *Nat. Commun.* **7**, 10793 (2016).
35. E. Strano, V. Nicosia, V. Latora, S. Porta, M. Barthélemy, Elementary processes governing the evolution of road networks, *Sci. Rep.* **2**, 296 (2012).
36. R. Louf, M. Barthélemy, A typology of street patterns, *J. R. Soc.SS Interface* **11**, 20140924 (2014).
37. R. Louf, M. Barthelemy, Modeling the polycentric transition of cities, *Phys. Rev. Lett.* **111**, 198702 (2013).
38. LandScan Global Population Database (2017); http://web.ornl.gov/sci/landscan/ [accessed 1 April 2017].
39. OpenStreetMap (2017); https://www.openstreetmap.org [accessed 1 April 2017].
40. Foursquare (2017); https://foursquare.com/ [accessed 15 April 2017].
41. J. L. Toole, S. Colak, B. Sturt, L. P. Alexander, A. Evsukoff, M. C. González, The path most traveled: Travel demand estimation using big data resources. *Transp. Res.Part C Emerg. Technol.* **58**, 162–177 (2015).
42. Y. Xu, M. C. González, Collective benefits in traffic during mega events via the use of information technologies. *J. R. Soc. Interface* **14**, 20161041 (2017).
43. D. Quercia, D. Saez, Mining urban deprivation from foursquare: Implicit crowdsourcing of city land use. *IEEE Pervasive Comput.* **13**, 30–36 (2014).
44. S. Spyratos, D. Stathakis, M. Lutz, C. Tsinaraki, Using foursquare place data for estimating building block use. *Environ. Plan. B Urban Anal. City Sci.* **44**, 693–717 (2017).
45. J. Frith, Communicating through location: The understood meaning of the foursquare check-in. *J. Comput. Mediated Commun.* **19**, 890–905 (2014).
46. R. Krueger, D. Thom, T. Ertl, Semantic enrichment of movement behavior with foursquare–A visual analytics approach. *IEEE Trans. Vis. Comput. Graph.* **21**, 903–915 (2015).
47. Y. Xu, S. Jiang, R. Li, J. Zhang, J. Zhao, S. Abbar, M. C. González, Unraveling environmental justice in ambient $PM_{2.5}$ exposure in Beijing: A big data approach. *Comput. Environ. Urban Syst.* **75**, 12–21 (2019).
48. A. Antunes, Á. Seco, N. Pinto, An accessibility–maximization approach to road network planning. *Comput. Aided Civ. Inf. Eng.* **18**, 224–240 (2003).
49. M. Barthélemy, Spatial networks. *Phys. Rep.* **499**, 1–101 (2011).

50. D. Levinson, Network structure and city size. *PLOS ONE* **7**, e29721 (2012).

51. M. G. Resende, R. F. Werneck, A fast swap-based local search procedure for location problems. *Ann. Oper. Res.* **150**, 205–230 (2007).

52. United States Census Bureau, Census data, (2016); https://www.census.gov/data.html. [accessed 15 Oct 2016].

53. A. Alhomaidhi, Geographic distribution of public health hospitals in Riyadh, Saudi Arabia. *Geogr. Bull.* **60**, 45–48 (2019).

54. R. H. M. Pereira, V. Nadalin, L. Monasterio, P. H. Albuquerque, Urban centrality: A simple index. *Geogr. Anal.* **45**, 77–89 (2013).

55. E. W. Dijkstra, A note on two problems in connexion with graphs. *Numer. Math.* **1**, 269–271 (1959).

56. D. Dohan, S. Karp, B. Matejek, *K-Median Algorithms: Theory in Practice* (Working Paper, Princeton, Computer Science, 2015).

57. M. Batty, P. Longley, *Fractal Cities: A Geometry of Form and Function* (Academica Press, 1994).

58. W. Alonso, *Location and Land Use* (Harvard Univ. Press, 1994).

59. E. S. Mills, B.-N. Song, *Urbanization and Urban Problems* (Harvard, 1979).

60. R. F. Muth, *Cities and Housing* (University of Chicago Press, 1969).

61. C. Clark, Urban population densities. *J. R. Stat. Soc.* **114**, 490–496 (1951).